



# Computational Modeling of Degradation of Substituted Benzyltrimethyl Ammonium

## Preprint

H. Long and B. S. Pivovar

*To be presented at the 226<sup>th</sup> Meeting of the Electrochemical Society  
Cancun, Mexico  
October 5–10, 2014*

**NREL is a national laboratory of the U.S. Department of Energy  
Office of Energy Efficiency & Renewable Energy  
Operated by the Alliance for Sustainable Energy, LLC**

This report is available at no cost from the National Renewable Energy Laboratory (NREL) at [www.nrel.gov/publications](http://www.nrel.gov/publications).

**Conference Paper**  
NREL/CP-2C00-62309  
September 2014

Contract No. DE-AC36-08GO28308

## NOTICE

The submitted manuscript has been offered by an employee of the Alliance for Sustainable Energy, LLC (Alliance), a contractor of the US Government under Contract No. DE-AC36-08GO28308. Accordingly, the US Government and Alliance retain a nonexclusive royalty-free license to publish or reproduce the published form of this contribution, or allow others to do so, for US Government purposes.

This report was prepared as an account of work sponsored by an agency of the United States government. Neither the United States government nor any agency thereof, nor any of their employees, makes any warranty, express or implied, or assumes any legal liability or responsibility for the accuracy, completeness, or usefulness of any information, apparatus, product, or process disclosed, or represents that its use would not infringe privately owned rights. Reference herein to any specific commercial product, process, or service by trade name, trademark, manufacturer, or otherwise does not necessarily constitute or imply its endorsement, recommendation, or favoring by the United States government or any agency thereof. The views and opinions of authors expressed herein do not necessarily state or reflect those of the United States government or any agency thereof.

This report is available at no cost from the National Renewable Energy Laboratory (NREL) at [www.nrel.gov/publications](http://www.nrel.gov/publications).

Available electronically at <http://www.osti.gov/scitech>

Available for a processing fee to U.S. Department of Energy and its contractors, in paper, from:

U.S. Department of Energy  
Office of Scientific and Technical Information  
P.O. Box 62  
Oak Ridge, TN 37831-0062  
phone: 865.576.8401  
fax: 865.576.5728  
email: <mailto:reports@adonis.osti.gov>

Available for sale to the public, in paper, from:

U.S. Department of Commerce  
National Technical Information Service  
5285 Port Royal Road  
Springfield, VA 22161  
phone: 800.553.6847  
fax: 703.605.6900  
email: [orders@ntis.fedworld.gov](mailto:orders@ntis.fedworld.gov)  
online ordering: <http://www.ntis.gov/help/ordermethods.aspx>

# Computational Modeling of Degradation of Substituted Benzyltrimethyl Ammonium

H. Long and B. S. Pivovar

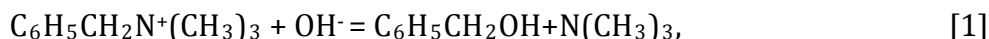
National Renewable Energy Laboratory, Golden, CO 80401, USA

The degradation of cations on the alkaline exchange membranes is the major challenge for alkaline membrane fuel cells. In this paper, we investigated the degradation barriers by density functional theory for substituted benzyltrimethyl ammonium (BTMA<sup>+</sup>) cations, which is one of the most commonly used cations for alkaline exchange membranes. We found that substituted cations with electron-releasing substituent groups at meta-position of the benzyl ring could result in improved degradation barriers. However, after investigating more than thirty substituted BTMA<sup>+</sup> cations with ten different substituent groups, the largest improvement of degradation barriers is only 1.6 kcal/mol. This implies that the lifetime of alkaline membrane fuel cells could increase from a few months to a few years by using substituted BTMA<sup>+</sup> cations, an encouraging but still limited improvement for real-world applications.

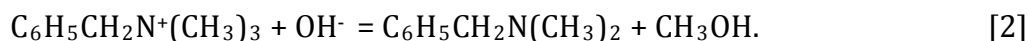
## Introduction

Alkaline fuel cell (AFC) is one of the oldest types of fuel cells<sup>1</sup> and has the advantage of enablement of cheaper, non-precious catalysts.<sup>2</sup> However, application of this type of fuel cell is still limited due to the carbonate salt precipitation formed on the electrodes when carbon dioxide from air reacts with alkaline electrolytes.<sup>3-4</sup> Researches on AFC have been renewed in recent years because of the development of the alkaline membrane fuel cells (AMFCs).<sup>5-6</sup> In an AMFC, an anion exchange membrane (AEM) is used between the electrodes to allow hydroxide (OH<sup>-</sup>) to transport across the membrane and prevents carbonate from forming precipitation. However, AEM degrades over time due to the reactions between OH<sup>-</sup> and the cations that are attached to the polymer backbone of the membrane, which is the major challenge for the AEFCs.<sup>6-8</sup>

Benzyltrimethyl ammonium (BTMA<sup>+</sup>) cation is the most commonly used cation in AEMs and has been investigated extensively for its application in AMFC.<sup>9-16</sup> Our experimental measurements had shown that the unsubstituted BTMA<sup>+</sup> cation degraded ~10% within 29 days in 5M NaOH at 80°C.<sup>10</sup> Two major degradation pathways for BTMA<sup>+</sup> are benzyl S<sub>N</sub>2 pathway and methyl S<sub>N</sub>2 pathway:<sup>17-18</sup>



and



Our density functional theory (DFT) calculations had shown that the transition state (TS) barriers ( $\Delta G^\ddagger$ ) for BTMA<sup>+</sup> benzyl S<sub>N</sub>2 pathway and methyl S<sub>N</sub>2 pathway were 23.3 kcal/mol and 25.1 kcal/mol respectively at 160°C and 1 atm.<sup>19</sup> Thus, the benzyl S<sub>N</sub>2 pathway is the dominant degradation pathway for BTMA<sup>+</sup>.

In order to further improve the stability of BTMA<sup>+</sup>, a straightforward method is to add substituent groups to the benzyl ring of BTMA<sup>+</sup>. In this manuscript, we modeled the BTMA<sup>+</sup> with different substituent groups at different positions and calculated degradation barriers using DFT method in order to search for cations with higher degradation barriers. To guide the search, we also investigated the relationship between  $\Delta G^\ddagger$  and Hammett substituents constants. We found that substituent -NRR' (where R and R' are alkyl groups) is the best type of substituents for improvement of the degradation barrier.

## Method

The detail method used for DFT calculations are described in our previous report.<sup>19</sup> In short, we use Gaussian 09 (G09)<sup>20</sup> to optimize the reactants and TS structures by B3LYP<sup>21</sup> method, 6-311++G(2d,p) basis set, and polarizable continuum solvation model (PCM). The free energies at 160° C and 1 atm for the reactants and TS were then calculated based on the optimized structure. The reaction free energy barrier  $\Delta G^\ddagger$  was then obtained by comparing the total free energies of the ground states of reactants (cation + OH<sup>-</sup>) with the free energy of the TS state.<sup>19</sup> During the calculations, no symmetry is used.

## Results

### Neutral substituents

We have computed  $\Delta G^\ddagger$  values of benzyl S<sub>N</sub>2 and methyl S<sub>N</sub>2 for substituted BTMA<sup>+</sup> cations at different positions on the benzene ring (Figure 1 and Table I). Five electron-releasing substituent groups and one electron-withdrawing substituent group, *i.e.*, -NO<sub>2</sub>, were investigated. For each substituent, we tried single substitutions at ortho, meta, and para positions (position 2, 3, and 4) and double substitutions at the meta positions (position 3 and 5).

Figure 1. Substituted BTMA<sup>+</sup> cations investigated in Section 3.1. X = -OH, -OCH<sub>3</sub>, -CH<sub>3</sub>, -NH<sub>2</sub>, -N(CH<sub>3</sub>)<sub>2</sub>, and -NO<sub>2</sub>.

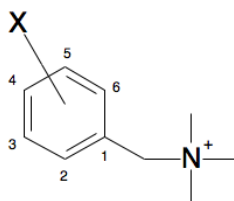


Table I.  $\Delta G^\ddagger$  values in kcal/mol of benzyl S<sub>N</sub>2 and methyl S<sub>N</sub>2 pathways for the unsubstituted and substituted BTMA<sup>+</sup> cations at 160°C and 1 atm. The one with a larger  $\Delta G^\ddagger$  than the unsubstituted BTMA<sup>+</sup> is shown in red.

Substitution Position	2(o)	3(m)	4(p)	3&5
-H (no substitution)	23.3/25.1			
-OH	20.2/25.1	23.4/24.7	23.4/25.5	23.8/24.5
-OCH <sub>3</sub>	24.6/26.1	22.9/25.6	23.8/26.3	23.8/25.0
-CH <sub>3</sub>	23.2/25.3	23.9/24.9	21.7/23.3	24.6/26.1
-NH <sub>2</sub>	22.0/25.4	23.1/25.3	23.0/26.3	24.9/25.4
-N(CH <sub>3</sub> ) <sub>2</sub>	24.1/26.5	24.5/25.1	22.0/27.8	24.9/26.9
-NO <sub>2</sub>	20.7/24.3	21.6/24.2	21.6/24.4	20.5/22.2

Figure 2.  $\Delta\Delta G^\ddagger$  values of (A) benzyl  $S_N2$  and (B) methyl  $S_N2$  for the substituted BTMA<sup>+</sup> cations compared with the unsubstituted BTMA<sup>+</sup>.

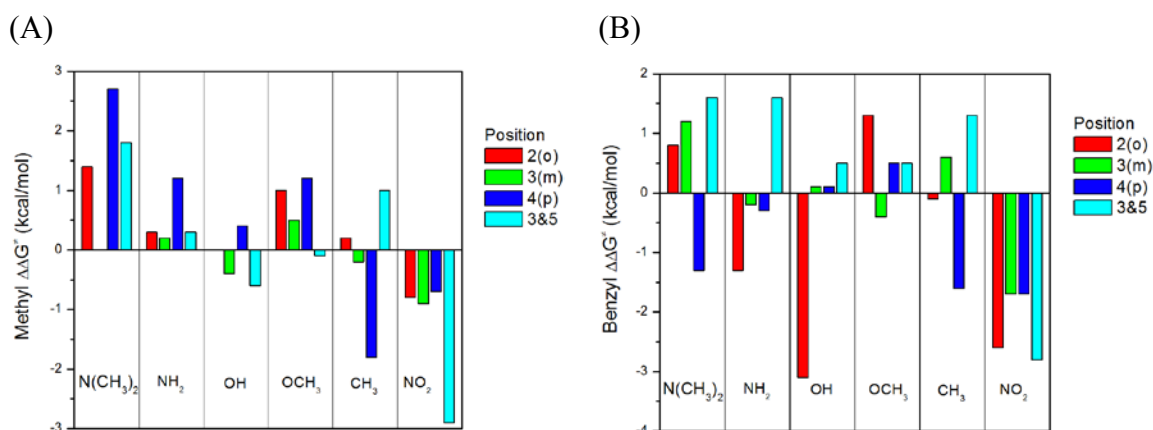


Figure 2 illustrates the  $\Delta\Delta G^\ddagger$  of the substituted BTMA<sup>+</sup> cations compared with the unsubstituted BTMA<sup>+</sup>. For the methyl  $S_N2$  reaction (Figure 2A), the  $\Delta\Delta G^\ddagger$  are between -3 ~ +3 kcal/mol. The  $\Delta\Delta G^\ddagger$  values for -N(CH<sub>3</sub>)<sub>2</sub> substitutions at all positions are  $\geq 0$  and the  $\Delta\Delta G^\ddagger$  values for all -NO<sub>2</sub> substitutions are  $< 0$ . The  $\Delta\Delta G^\ddagger$  for other substituted cations are either larger or smaller than 0, depending on the substitution positions. The largest  $\Delta\Delta G^\ddagger$  is 2.7 kcal/mol from the para -N(CH<sub>3</sub>)<sub>2</sub> substitution.

For the benzyl  $S_N2$  reaction (Figure 2B), the  $\Delta\Delta G^\ddagger$  are between -3 ~ +2 kcal/mol. The largest  $\Delta\Delta G^\ddagger$  is 1.6 kcal/mol from the double-meta substituted -NH<sub>2</sub> and -N(CH<sub>3</sub>)<sub>2</sub>. Again, the  $\Delta\Delta G^\ddagger$  values for all -NO<sub>2</sub> substitutions are less than 0. For all of the substitutions, the  $\Delta\Delta G^\ddagger$  values of benzyl  $S_N2$  are always smaller than the methyl ones, indicating that the methyl  $S_N2$  reaction is always not the rate-limiting step for the degradation of the substituted BTMA<sup>+</sup> cations. All of the benzyl  $S_N2$   $\Delta\Delta G^\ddagger$  values for the double-meta substitutions with electron-releasing substituent groups are larger than the unsubstituted BTMA<sup>+</sup>, indicating that this type of substitutions is promising candidate cations with higher stability.

## $\Delta G^\ddagger$ and Hammett substituent constants

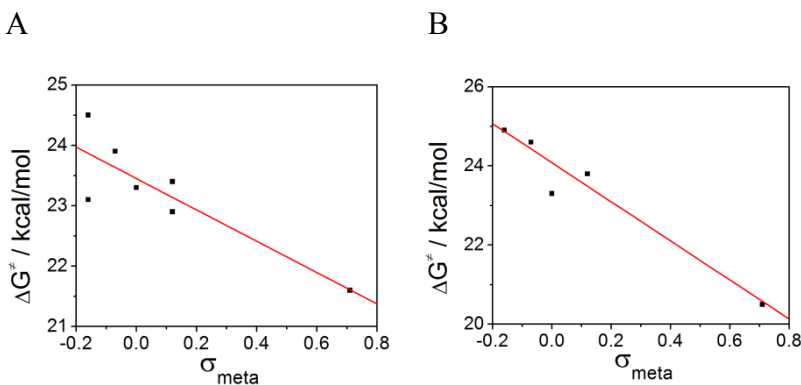
The correlation between  $\Delta G^\ddagger$  and substituent groups could be described by the Hammett equation where  $\Delta G^\ddagger$  has a linear relationship with the Hammett substituent constants  $\sigma$ .<sup>22-23</sup> Values of  $\sigma$  depend on the substituent groups and the substitution positions. For the neutral para substitutions, when the reaction TS structure has positive or negative charges,  $\sigma_{\text{para}}^+$  or  $\sigma_{\text{para}}^-$  values should be used instead of  $\sigma_{\text{para}}$ .<sup>23</sup> Table II presents the Hammett substituent constants compiled by Hansch *et al*.<sup>23</sup> Figure 3 and 4 illustrate the plots of  $\Delta G^\ddagger$  vs.  $\sigma$ .

Table II. The Hammett substituent constants from Hansch *et al*.<sup>23</sup>

Substitution Position	$\sigma_{\text{meta}}$	$\sigma_{\text{para}}$	$\sigma_{\text{para}}^+$	$\sigma_{\text{para}}^-$
-H (no substitution)		0		
-OH	0.12	-0.37	-0.92	-0.37
-OCH <sub>3</sub>	0.12	-0.27	-0.78	-0.26
-CH <sub>3</sub>	-0.07	-0.17	-0.31	-0.17
-NH <sub>2</sub>	-0.16	-0.66	-1.3	-0.15
-N(CH <sub>3</sub> ) <sub>2</sub>	-0.16	-0.83	-1.7	-0.12
-NO <sub>2</sub>	0.71	0.78	0.79	1.27

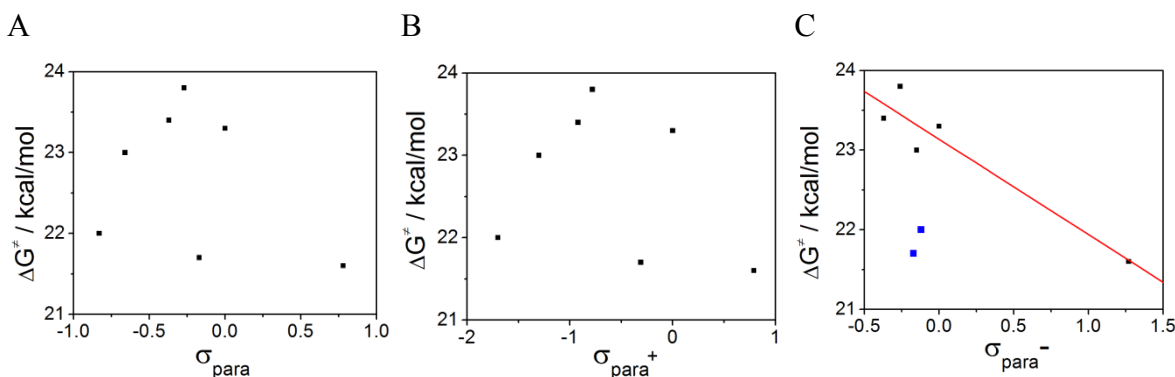
For the meta substitutions, the  $\Delta G^\ddagger$  vs.  $\sigma_{\text{meta}}$  plot (Figure 3A) shows a linear relationship. The linear regression analysis results in a slope of -2.6 kcal/mol with the coefficient of determination  $R = 0.87$ . For the double-meta substitutions, because -OH and -OCH<sub>3</sub> have the same  $\Delta G^\ddagger$  and  $\sigma_{\text{meta}}$  values, and -NH<sub>2</sub> and -N(CH<sub>3</sub>)<sub>2</sub> have the same  $\Delta G^\ddagger$  and  $\sigma_{\text{meta}}$  values, only five data points are shown on Figure 3B. The slope for Figure 3B is -4.9 kcal/mol, almost double the values of Figure 3A, indicating that double-meta substitutions result in a stronger stabilization effect (or destabilization effect for -NO<sub>2</sub>) from the substituent groups. The  $R$ -value for this fit is 0.97, showing a much better linear relationship than the single-meta substitution case.

Figure 3.  $\Delta G^\ddagger$  as a function of  $\sigma_{\text{meta}}$  for (A) single-meta substitutions and (B) double-meta substitutions. The red trend lines are fitted by linear regression.



For the para substitutions, the  $\Delta G^\ddagger$  vs.  $\sigma_{\text{para}}$  plot (Figure 4A) shows no linear relationship. Since the cations are charged, we also made plots for  $\Delta G^\ddagger$  vs.  $\sigma_{\text{para}}^+$  (Figure 4B) and  $\Delta G^\ddagger$  vs.  $\sigma_{\text{para}}^-$  (Figure 4C). Only Figure 4C shows somewhat linear relationship but two data points are still far from the trend line (in blue color). These two points are from  $-\text{CH}_3$  and  $-\text{N}(\text{CH}_3)_2$ . The TS structure of the benzyl  $\text{S}_{\text{N}}2$  reaction for the  $\text{BTMA}^+$  cation is neutral and the cation is positively charged. This case is similar to the reaction with a negatively charged TS structure and a neutral reactant, in which the TS structure has more negative charge than the reactant, which may be the reason that the  $\sigma_{\text{para}}^-$  results in the best linear relationship. If the two data points far from the trend line are omitted, a slope of -1.2 kcal/mol is obtained from the linear regression.

Figure 4.  $\Delta G^\ddagger$  as a function of (A)  $\sigma_{\text{para}}$ , (B)  $\sigma_{\text{para}}^+$ , and (C)  $\sigma_{\text{para}}^-$  for para substitutions. In C, only the black data points were used to fit the red trend line.



### Multiple-charged $\text{BTMA}^\pm$

The substituent group itself could have positive charges, resulting in a cation with multiple positive charges. We calculated the benzyl  $\text{S}_{\text{N}}2$   $\Delta\Delta G^\ddagger$  of  $-\text{CH}_2\text{N}^+(\text{CH}_3)_3$  substituted  $\text{BTMA}^+$  cations. The ortho, meta, and para substitutions have benzyl  $\text{S}_{\text{N}}2$   $\Delta\Delta G^\ddagger$  values of -1.8 kcal/mol, -3.4 kcal/mol and -1.2 kcal/mol respectively, when compared to the unsubstituted  $\text{BTMA}^+$  cation. Obviously, substituted  $\text{BTMA}^+$  cations with multiple-charge centers will have smaller  $\Delta G^\ddagger$  values than the unsubstituted  $\text{BTMA}^+$  due to the strong charge-charge repulsion. Therefore, for cations with high stability, the substituent groups should be neutral.

### Double-meta substitutions by $-\text{NRR}'$

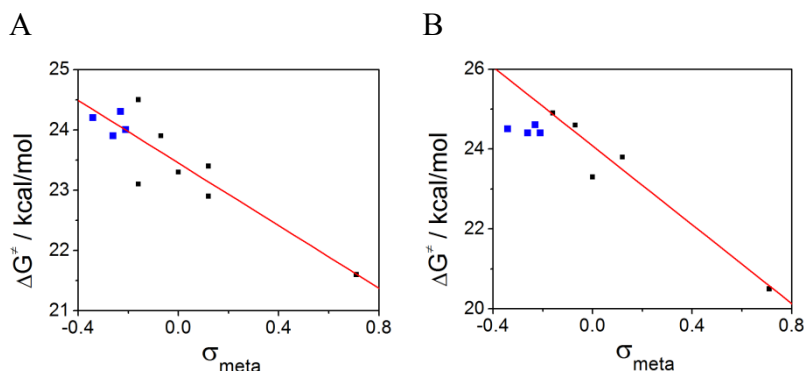
Encouraged by the large benzyl  $\text{S}_{\text{N}}2$   $\Delta\Delta G^\ddagger$  values of  $-\text{NH}_2$  and  $-\text{N}(\text{CH}_3)_2$ , we further investigated substituent groups in  $-\text{NRR}'$  form at meta and double-meta positions. We studied four substituent groups with large negative  $\sigma_{\text{meta}}$  values and expected them to have improved degradation barriers. The four substituent groups are:  $-\text{N}(\text{CH}_2\text{CH}_3)_2$ ,  $-\text{N}(\text{CH}_2\text{CH}_2\text{CH}_3)_2$ ,  $-\text{NH}(\text{CH}_3)$ , and  $-\text{NH}(\text{CH}_2\text{CH}_2\text{CH}_2\text{CH}_3)$ . Table III presents their  $\sigma_{\text{meta}}$  values<sup>23</sup> and calculation results. Although they all show some improvement when compared to the unsubstituted  $\text{BTMA}^+$ , none of them has a benzyl  $\text{S}_{\text{N}}2$   $\Delta G^\ddagger$  larger than the one of double-meta  $-\text{N}(\text{CH}_3)_2$ , which is 24.9 kcal/mol. Figure 5 shows the case that the corresponding four data points are added to the plots of Figure 3. Although these points still follow the trend lines, in some case, the deviations from the trend lines are

more than 0.5 kcal/mol. This suggests that we could use the Hammett substituent constants to roughly estimate the benzyl  $S_N2$   $\Delta G^\ddagger$ , however, the predictions made by this method are still not accurate enough to guide us in search for cations with even higher degradation barriers.

Table III.  $\Delta G^\ddagger$  values in kcal/mol of benzyl  $S_N2$ /methyl  $S_N2$  for -NRR' substituted BTMA<sup>+</sup> cations at 160°C and 1 atm.

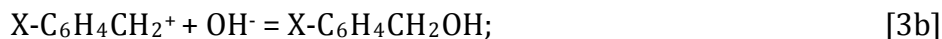
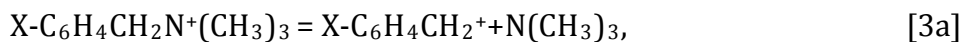
	$\sigma_{\text{meta}}$	3-substitution $\Delta G^\ddagger$	3&5 substitution $\Delta G^\ddagger$
-N(CH <sub>2</sub> CH <sub>3</sub> ) <sub>2</sub>	-0.23	24.3/27.4	24.6/26.3
-N(CH <sub>2</sub> CH <sub>2</sub> CH <sub>3</sub> ) <sub>2</sub>	-0.26	23.9/25.7	24.4/25.7
-NH(CH <sub>3</sub> )	-0.21	24.0/26.2	24.4/26.1
-NH(CH <sub>2</sub> CH <sub>2</sub> CH <sub>2</sub> CH <sub>3</sub> )	-0.34	24.2/25.7	24.5/25.9

Figure 5.  $\Delta G^\ddagger$  as a function of  $\sigma_{\text{meta}}$  for (A) single-meta substitutions and (B) double-meta substitutions. The four blue data points are for -NRR' substituted BTMA<sup>+</sup> reported in this section and were not used to fit the red trend line.

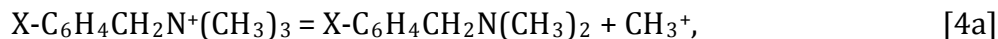


### $S_N1$ pathway

Besides the benzyl and methyl  $S_N2$  pathways, BTMA<sup>+</sup> may also take the benzyl  $S_N1$  pathway,



and the methyl  $S_N1$  pathway,



where X is the substituent group. For the unsubstituted BTMA<sup>+</sup>, these degradation pathways were not investigated in previous reports because reaction barriers for reactions [3a] and [4a] are obviously very high in aqueous solution owing to the formation of the highly unstable  $\text{CH}_3^+$  and  $\text{C}_6\text{H}_5\text{CH}_2^+$  cations. However, when there are one or more



electron-releasing substituent groups on the benzyl ring, the  $X-C_6H_4CH_2^+$  cation is stabilized, which may result in a relatively lower reaction barrier for reaction [3a]. Table IV presents the benzyl  $S_N1$   $\Delta G^\ddagger$  of select cations. For the unsubstituted  $BTMA^+$ , benzyl  $S_N1$   $\Delta G^\ddagger$  is 33.2 kcal/mol, much larger than the benzyl  $S_N2$   $\Delta G^\ddagger$  23.3 kcal/mol. This is consistent with previous conclusion that benzyl  $S_N2$  pathway is the dominant degradation pathway.<sup>17, 19, 24-25</sup> For the double-meta  $-OCH_3$  substitution, the benzyl  $S_N1$   $\Delta G^\ddagger$  is 32.6 kcal/mol, close to one of the unsubstituted  $BTMA^+$ . For the double-meta  $-N(CH_3)_2$  substitution, the benzyl  $S_N1$   $\Delta G^\ddagger$  is 27.7 kcal/mol, still larger than its benzyl  $S_N2$   $\Delta G^\ddagger$  (24.9 kcal/mol), although the gap between  $S_N1$   $\Delta G^\ddagger$  and  $S_N2$   $\Delta G^\ddagger$  is much smaller. The stabilization effect is much stronger for electron-releasing substituents at ortho and para positions. The para  $-N(CH_3)_2$  has a benzyl  $S_N1$   $\Delta G^\ddagger$  as small as 11.3 kcal/mol, much smaller than its benzyl  $S_N2$   $\Delta G^\ddagger$ , 22.0 kcal/mol. For the double-ortho  $-OCH_3$  substitution, it has a relative large benzyl  $S_N2$   $\Delta G^\ddagger$ , 24.1 kcal/mol, but its benzyl  $S_N1$   $\Delta G^\ddagger$  is only 20.6 kcal/mol. In both cases, the benzyl  $S_N1$  pathway becomes the dominant degradation pathway, and thus, the rate-limiting step for the degradation. Therefore, in search for the  $BTMA^+$  derivative cations with high stability, meta substitutions with electron-releasing substituents are preferred, not only because meta substitutions have larger benzyl  $S_N2$   $\Delta G^\ddagger$ , but also because ortho and para substitutions may have relatively small benzyl  $S_N1$   $\Delta G^\ddagger$ .

Table IV.  $\Delta G^\ddagger$  values in kcal/mol of benzyl  $S_N1$  and  $S_N2$  pathways for the unsubstituted and select substituted  $BTMA^+$  cations at 160°C and 1 atm.

	-H	-OCH <sub>3</sub>	-N(CH <sub>3</sub> ) <sub>2</sub>	-N(CH <sub>3</sub> ) <sub>2</sub>	-OCH <sub>3</sub>
Position	N/A	3&5	3&5	4	2&6
Benzyl $S_N1$ $\Delta G^\ddagger$	33.2	32.6	27.7	11.3	20.6
Benzyl $S_N2$ $\Delta G^\ddagger$	23.3	23.8	24.9	22.0	24.1

## Conclusions

According to our calculation results, we could conclude that methyl  $S_N2$  pathway is not the rate-limiting step of degradation for substituted  $BTMA^+$  cations. Double-meta substitutions with electron-releasing substituent groups result in improved stability for the benzyl  $S_N2$  pathway. For cations with electron-releasing substituents, especially for those with substituents at ortho and para positions, the barrier of benzyl  $S_N1$  pathway could be low enough to become the rate-limiting step. In addition, positively charge substituent groups will decrease the stability of cations. We also found that although Hammett substituent constants could be used to predict the degradation barrier, these predictions were not accurate enough to guarantee a high degradation barrier.

We noted that some of the substituted  $BTMA^+$  cations would be very difficult to synthesize and/or purify experimentally, for example, the ones with  $-OH$ ,  $-NH_2$ , or  $-NRR'$ . The most important finding of this computational work, however, is that substituted  $BTMA^+$  cations show less than one magnitude of improvement on stability. Although we have investigated degradation barriers for more than thirty cations with ten

different substituent groups, the cation with the largest improvement found in this manuscript, that is, the one with double-meta  $-\text{N}(\text{CH}_3)_2$ , only has a  $\Delta\Delta G^\ddagger$  of 1.6 kcal/mol at 160°C. At a temperature of 80°C, which is the typical working temperature of a fuel cell, our calculation shows that its  $\Delta\Delta G^\ddagger$  is 1.5 kcal/mol. According to the transition state theory, degradation reaction rate constant  $k \propto \exp(-\Delta\Delta G^\ddagger/RT)$ , where  $R$  is the gas constant and  $T$  is the temperature. A  $\Delta\Delta G^\ddagger$  of 1.5 kcal/mol will result in a decrease in degradation rate of 8.5 times at 80°C. Our experimental work had shown that unsubstituted BTMA<sup>+</sup> cation degrades ~10% within 29 days in 5M NaOH at 80°C.<sup>10</sup> Thus, it could be predicted that for the double-meta  $-\text{N}(\text{CH}_3)_2$  substituted BTMA<sup>+</sup>, it would degrades ~10% within ~8 months. This degradation rate implies that an AEMFC with a lifetime of a few years could be built, much better than the AEMFC using the unsubstituted BTMA<sup>+</sup>, which would only have a lifetime in months, and this might be useful for some real-world applications. However, in order to build fuel cell vehicles with a comparable lifetime of conventional ones, this is still far from sufficient. Therefore, our calculation results suggest that the improvement of the BTMA<sup>+</sup> stability by adding substituent groups to the benzyl ring is limited. In search for even larger improvement of cation stability, other types of cations should be investigated. Our recent calculation results indicated that substituted imidazolium cations may have several magnitudes of improvement of stability over the BTMA<sup>+</sup> cation and thus are more promising than BTMA<sup>+</sup> derivative cations.<sup>26</sup>

### Acknowledgements

This work was supported by the U.S. Department of Energy, Office of Basic Energy Sciences, Division of Materials Science and Engineering, under Contract No. DE-AC36-08-GO28308. This research used capabilities of the National Renewable Energy Laboratory Computational Science Center, which is supported by the Office of Energy Efficiency and Renewable Energy of the U.S. Department of Energy.

### References

1. J. M. Andujar and F. Segura, *Renew Sust Energ Rev*, **13**(9), 2309 (2009).
2. E. Gulzow, *J Power Sources*, **61**(1-2), 99 (1996).
3. E. Gulzow and M. Schulze, *J Power Sources*, **127**(1-2), 243 (2004).
4. G. F. McLean, T. Niet, S. Prince-Richard and N. Djilali, *Int J Hydrogen Energ*, **27**(5), 507 (2002).
5. J. R. Varcoe and R. C. T. Slade, *Fuel Cells*, **5**(2), 187 (2005).
6. G. Couture, A. Alaaeddine, F. Boschet and B. Ameduri, *Prog Polym Sci*, **36**(11), 1521 (2011).
7. C. S. Macomber, J. M. Boncella, B. S. Pivovar and J. A. Rau, *J Therm Anal Calorim*, **93**(1), 225 (2008).
8. Joseph B Edson, Clay S. Macomber, Bryan S. Pivovar and James M. Boncella, *J Membrane Sci*, **399-400**, 49 (2012).
9. J. R. Varcoe, R. C. T. Slade and E. Lam How Yee, *Chem Commun*, (13), 1428 (2006).
10. B.R. Einsla, S. Chempath, L.R. Pratt, J. R. Boncella, C. Macomber and B. S. Pivovar, *ECS Transactions*, **11**(1), 1173 (2007).

11. E. N. Komkova, D. F. Stamatialis, H. Strathmann and M. Wessling, *J Membrane Sci*, **244**(1-2), 25 (2004).
12. O. I. Deavin, S. Murphy, A. L. Ong, S. D. Poynton, R. Zeng, H. Herman and J. R. Varcoe, *Energ Environ Sci*, **5**(9), 8584 (2012).
13. C. G. Arges, J. Parrondo, G. Johnson, A. Nadhan and V. Ramani, *J Mater Chem*, **22**(9), 3733 (2012).
14. C. G. Arges and V. Ramani, *J Electrochem Soc*, **160**(9), F1006 (2013).
15. C. G. Arges and V. Ramani, *P Natl Acad Sci USA*, **110**(7), 2490 (2013).
16. C. Fujimoto, D. S. Kim, M. Hibbs, D. Wroblewski and Y. S. Kim, *J Membrane Sci*, **423**, 438 (2012).
17. S. Chempath, J. M. Boncella, L. R. Pratt, N. Henson and B. S. Pivovar, *J Phys Chem C*, **114**(27), 11977 (2010).
18. S. Chempath, B. R. Einsla, L. R. Pratt, C. S. Macomber, J. M. Boncella, J. A. Rau and B. S. Pivovar, *J Phys Chem C*, **112**(9), 3179 (2008).
19. H. Long, K. Kim and B. S. Pivovar, *J Phys Chem C*, **116**(17), 9419 (2012).
20. M. J. Frisch, G. W. Trucks, H. B. Schlegel, G. E. Scuseria, M. A. Robb, J. R. Cheeseman, G. Scalmani, V. Barone, B. Mennucci and G. A. Petersson et al, *Gaussian, Inc., Gaussian 09, Revision A.02, Wallingford CT*, (2009).
21. A. D. Becke, *J Chem Phys*, **98**(7), 5648 (1993).
22. Louis P. Hammett, *J. Am. Chem. Soc.*, **59**(1), 96 (1937).
23. C. Hansch, A. Leo and R. W. Taft, *Chem Rev*, **91**(2), 165 (1991).
24. Elizabeth W. Baumann, *J. Chem. Eng. Data*, **5**(3), 376 (1960).
25. Melvin J. Hatch and Winston D. Lloyd, *Journal of Applied Polymer Science*, **8**(4), 1659 (1964).
26. H. Long and B. S. Pivovar, *J. Phys. Chem. C*, **118**(19), 9880 (2014).